



The Skylab Brazing Experiment

Stainless steel and nickel specimens brazed in near-zero gravity aboard Skylab exhibit fewer voids and less small defects than identical specimens processed on Earth

T. A. SIEWERT, R. W. HEINE, C. M. ADAMS, JR., AND J. R. WILLIAMS

ABSTRACT. Four specimens from the M552 Exothermic Brazing Experiment processed aboard Skylab in June 1973 have been compared to identical samples processed on Earth under conditions duplicating as much as possible those of the Skylab-processed samples except for the gravitational field.

These samples simulated a butt joint of 1.91 cm (0.750 in.) tubes in a concentric sleeve with electrically ignited exothermic material for melting the preplaced braze filler metal. Samples varied in gap dimension (0.13 to 0.75 mm, 0.005 to 0.029 in.) and material (304L stainless steel and 99.999% nickel). The two nickel samples contained a radioactive tracer for determination of filler metal flow modes.

Comparison of radiographs of the Skylab and ground-processed samples revealed the Skylab samples had a generally lower concentration of voids and less small defects in the filler metal. All the Skylab samples had braze gaps filled to at least the same extent as the ground samples. Brazing was thus demonstrated to be an effective method of joining in near-zero gravity.

The microstructures of the Skylab and ground-processed samples contained some striking differences. The

greater freedom for flow in the absence of gravity is advanced as the explanation for the higher concentration of base metal particles dispersed in the filler metal of the Skylab samples. Partitioning of copper was observed in the filler metal of one Skylab sample.

Introduction

Skylab Chronology

The Exothermic Brazing Experiment was proposed late in 1965 as the Marshall Space Flight Center (MSFC) No. 35 experiment for the Saturn IV-B Workshop. In September 1966, it was

Paper presented at the 8th International AWS Brazing Conference held in Philadelphia, Pennsylvania, on April 26-28, 1977.

T. A. SIEWERT is Supervising Research Engineer, Chemetron Corporation, Gases Group Research Center, Hanover, Pennsylvania, and was formerly Research Associate, Dept. of Metallurgical and Mineral Engineering, University of Wisconsin-Madison; R. W. HEINE is Professor, Dept. of Metallurgical and Mineral Engineering, University of Wisconsin-Madison; C. M. ADAMS, JR., is Dean, College of Engineering, University of Cincinnati, Cincinnati, Ohio; and J. R. WILLIAMS is Deputy Chief, Process Engineering Division, Marshall Space Flight Center, NASA, Huntsville, Alabama.

approved as Experiment M492, Tube Joining in Space. The initiation of the proposal was motivated by Air Force programs with exothermic heating sources which could be operated at pressures as low as $13.3322 \times 10^{-3} \text{ N/m}^2$ (10^{-6} Torr). In the ensuing years, under contracts with the Whittaker Corporation, exothermic material compositions and configurations were developed for the M492 experiment and verified by extensive testing at Marshall Space Flight Center.

In 1968, the M492 experiment was re-evaluated and approved by NASA as the Exothermic Brazing task of the M512 series of experiments. Later, the experiment number and name were changed to the M552 Exothermic Brazing Experiment. Qualification and hardware testing continued through 1972, preparing the experiment for the 1973 Skylab flight. On June 12 and 13, 1973, Astronaut Paul J. Weitz processed four braze specimens on NASA's Earth-Orbiting Skylab.

M-552 Exothermic Brazing Experiment

The Marshall Space Flight Center developed a series of Materials-Processing-in-Space experiments for the Skylab flight for the specific goal of obtaining data leading to: "(1) the capability to fabricate and repair struc-

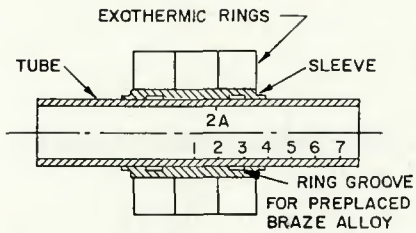


Fig. 1—Cross-section of sample used in the Skylab brazing experiments (about 50% actual size)

tures in space, (2) the development of unique or improved materials for use on Earth, and (3) the acquisition of new knowledge of material properties and performance.¹

The M-552 Exothermic Brazing Experiment was one in this series. It consisted of preparing four samples of the configuration shown in Fig. 1 for processing in space on the Skylab flight during June 1973 and subsequent comparison of these Skylab-processed samples with identical ground characterization samples processed on Earth. Ground characterization samples were processed under conditions duplicating as closely as possible those of the Skylab-processed samples, except for the gravitational field.

Stainless steel was chosen as the material for two of the gap configurations, because it is a common commercial structural material often joined by brazing. SLS-1, the narrow 0.13 mm (0.005 in.) gap, was chosen at the normal upper limit of gap spacing for common brazing practice. In comparison, SLS-3, with a wide 0.5 mm (0.020 in.) gap, was chosen beyond this limit with insufficient alloy to fill the

gap. In this wide gap, the resultant distribution of braze alloy was expected to provide information on the effect of gravity on filling of the gap and evidence of change in menisci formed on freezing.²

Nickel was chosen as the other material for the other two samples to provide information on braze alloying in an entirely different system, one with little commercial use but of great scientific interest. The narrow gap sample SLN-2, 0.25 mm (0.010 in.), was chosen to barely fill on Earth, and the taper gap sample SLN-4, 0-0.75 mm (0-0.030 in.), was designed to fill only partially to study the effect of gravity on the final distribution of metal.²

For each of the four Skylab configurations, there were three identical samples processed in a vacuum cham-

ber on Earth under brazing conditions duplicating those aboard Skylab with the exception of gravity. Sectioning and analysis of these samples provided the ground-based characterization necessary for the evaluation of the effect of the near-zero gravity on the Skylab samples.

Experimental Procedure

A cylindrical sleeve with machined grooves for preplaced braze alloy was positioned concentric with a 19.1 mm (0.750 in.) inner tube—Fig. 1. The sleeve was surrounded by an electrically fired exothermic material which heated the sample to brazing temperatures, where the preplaced braze alloy melted and flowed into the narrow gap between the tube and sleeve.²

Each specimen possessing a different clearance gap between the tube and sleeve was positioned in a separate canister containing the exothermic material, ignitors and insulation. This assembly is shown in Fig. 2. Two of the four specimens contained pure nickel tubes and sleeves. An isotope, silver-110 with a half-life of 253 days, was added to a section of one braze ring in the nickel specimens to enhance analysis of capillary flow. The location of the isotope pellet prior to melting is shown in Fig. 3. The other two tubes and sleeves were type 304L stainless steel with the tube partially slit through the center cross-section to simulate a butt joint. Sample identification material and gap clearances between the sleeves and tubes are noted in Table 1.²

Each braze alloy ring weighed 1.95 grams and was composed of 71.8 wt % silver, 28.0 wt % copper and 0.2 wt % lithium. The alloy's melting temperature was 760 C (1410 F).

Three exotherm rings with a combined weight of 60 grams were

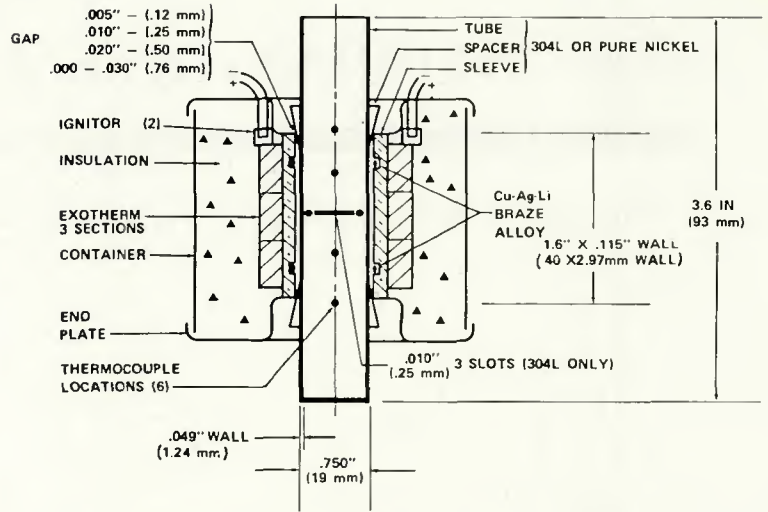
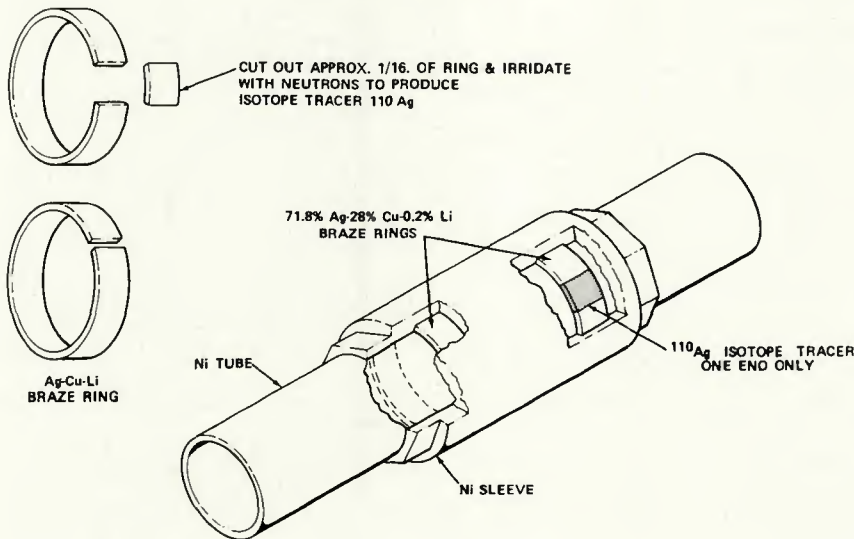


Fig. 2—Cross-section of tube and sleeve assembly in brazing container

M552 ISOTOPE TRACER



APPLICATION—NICKEL SAMPLES WITH .010" & .000"-.030" GAP

Fig. 3—Isotope location—nickel samples

Table 1—Brazing Specimen Specifications

Exotherm heaters	Application	Brazed at	Tube position	Type material	Isotope tracer	Thermal profile	Gap dimension	Identification	
1	Astronaut training stainless	MSFC ^(a)	Horizontal	347			0.05 mm (0.002 in.)	AT 5	
2								AT 6	
3								AT 7	
4								AT 8	
5	Metallurgical characterization stainless	MSFC	Horizontal	304L		X	0.13 mm (0.005 in.)	MCS 1	
6						X	0.13 mm (0.005 in.)	MCS 2	
7							0.13 mm (0.005 in.)	MCS 3	
8							0.50 mm (0.020 in.)	MCS 4	
9							0.50 mm (0.020 in.)	MCS 5	
10							0.50 mm (0.020 in.)	MCS 6	
11 Exotherm	Metallurgical characterization stainless	M5FC	Horizontal	Ni	X@ 12:00	X	0.25 mm (0.010 in.)	MCN 1	
12 Material			Horizontal		X@ 3:00	X	0.25 mm (0.010 in.)	MCN 2	
13 Jan. and			Horizontal		X@ 6:00		0.25 mm (0.010 in.)	MCN 3	
14 June 1971			Vertical		X@ bottom		0-0.75 mm (0-0.030 in.)	MCN 4	
15			Vertical		X@ bottom		0-0.75 mm (0-0.030 in.)	MCN 5	
16			Vertical		X@ bottom		0-0.75 mm (0-0.030 in.)	MCN 6	
17	Isotope mapping	M5FC	Horizontal	Ni	X@ 3:00		0.25 mm (0.010 in.)	IMN 1	
18			Vertical	Ni	X@ bottom		0-0.75 mm (0-0.030 in.)	IMN 2	
19	Thermal flow data	MIT ^(b)	Horizontal	347			0.05 mm (0.002 in.)	TF 1	
20								TF 2	
21								TF 3	
1	Skylab flight samples	Skylab	NA ^(b)	304L	X		0.13 mm (0.005 in.)	SLS 1	
2				Ni				0.25 mm (0.10 in.)	SLN 2
3				304L				0.50 mm (0.020 in.)	SLS 3
4				Ni				0-0.75 mm (0-0.030 in.)	SLN 4
5 Exotherm	Skylab backup samples	To Be Determined	NA ^(b)	304L	X		0.13 mm (0.005 in.)	SBS 1	
6 Material				Ni				0.25 mm (0.010 in.)	SBN 2
7 Dec. 1972				304L				0.50 mm (0.020 in.)	SBS 3
8				Ni				0-0.75 mm (0-0.030 in.)	SBN 4

^(a)MSFC—Marshall Space Flight Center; MIT—Massachusetts Institute of Technology
^(b)NA—Not available

installed over the sleeve as the heat source required to produce a brazed tube and sleeve joint. Substantially all of the reaction products were solid, and no external oxygen supply was required for the reaction. The exothermic material ignites at 1104 C (2020 F) and produces 650 calories per gram. Approximately 90 seconds are required for the exotherm to complete its reaction. The exotherm used in the M552 experiment had the following composition: aluminum—24.8%; boron—5.0%; titanium dioxide—55.2%; vanadium pentoxide—15.0%.

Two ignitors positioned against the exotherm ring were used to initiate the exothermic reaction. Although one ignitor is normally sufficient, the second one was added to provide redundancy to the system. This ignitor exothermic material reacts at 510 C (950 F) and has the following composition: aluminum—14.8%; boron—7.7%; titanium—10.0%; vanadium pentoxide—67.5%.

The exothermic material was surrounded with Fiberflax (fibrous aluminum oxide) insulating material, which contained the heat generated for the

brazing process and also protected the outside container from overheating.

The aluminum housing which held the four exothermic brazing packages was made in two halves and, after installation of four exothermic packages, was bolted together on the line shown along its median plane in Fig. 4. A thermocouple temperature sensor was bolted onto the top portion of the housing. Electrical connections to this sensor and to the ignitor wires in the exothermic packages were soldered to an insulated terminal board also attached to the top section of the

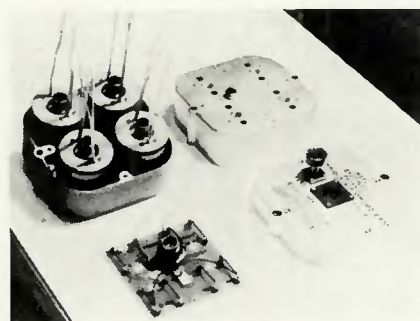


Fig. 4—Housing assembly and contents

housing. All electrical connections were led out of the case through the power connector on the cover. Figure 5 shows a schematic of the total exothermic assembly during final assembly of all major components, including the brazing packages and the terminal board.

Power for initiation of the exothermic reactions was provided by the 28 V batteries contained in the M512 facility and controlled through selector and trigger switches on the facility's control panel within the Skylab's Multiple Docking Adaptor (MDA). Each initiating pulse was 120 amperes at 28 volts for 5 milliseconds (14.4 watt seconds per pulse). The temperature sensor output on the M512 chamber was read on the control panel's temperature gauge. The thermocouple sensor closes a circuit at approximately 43.3 C (110 F), and this action was displayed by a hot light indicator on the control panel.

Thermal Regime

Information was obtained on the reproducibility of the exothermic ma-

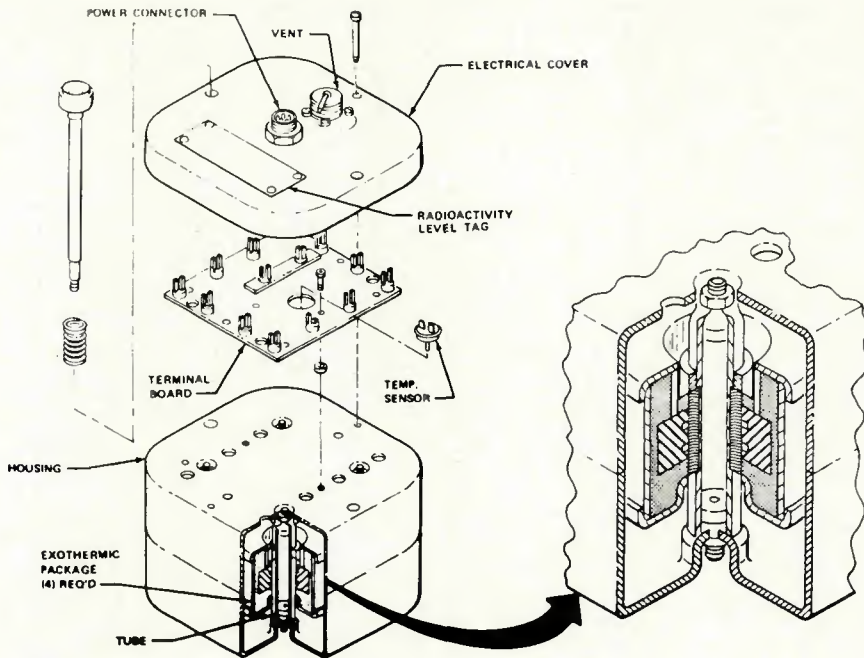


Fig. 5—Assembly of M552 exothermic package

terial via a thermocouple attached to the inside of the tube of all ground samples. This data, presented in Table 2, was needed to observe the effect of temperature on the severity of braze alloy interaction with the tube and sleeve.

To determine the time-temperature cycle, thermocouples were placed at seven positions along the inside of the tube at locations indicated by numbers 1 through 7 in Fig. 1. These thermocouples produced the temperature data shown in Fig. 6.

Further studies were conducted by drilling holes through the tube and placing a thermocouple on the interior surface of the sleeve with another placed adjacent to the hole on the interior surface of the tube. These tests were performed at locations near the ring groove and 180° around the circumference of the tube, shown as locations 2 and 2A respectively in Fig. 1. These thermocouples produced the data of Fig. 7. Measurements were

made of the braze alloy surface tension at various temperatures for use in calculations of expected zero gravity effects.^{8,9}

Ground-Based Processing

Ground processing consisted of two types of tests, one to provide ground reference for the Skylab flights and to test analysis procedures, and the other type to study and attempt to reproduce structures observed on the Skylab flights. These flights were not necessarily of the Skylab configuration.

Skylab Reference and Procedural Samples

Twelve specimens of flight configuration were brazed at Marshall Space Flight Center prior to the flight experiment.² A typical laboratory test setup is shown in Fig. 8. These brazed specimens served as radiographic and metallographic references for compar-

Table 2—Maximum Temperatures Reached on Ground Comparison Specimens

Identification	Configuration	Maximum temperature
MCS-1	0.13 mm (0.005 in.) Stainless Steel	1045 C (1913 F)
MCS-2	0.13 mm (0.005 in.) Stainless Steel	1045 C (1913 F)
MCS-3	0.13 mm (0.005 in.) Stainless Steel	990 C (1814 F)
MCS-4	0.5 mm (0.020 in.) Stainless Steel	1035 C (1895 F)
MCS-5	0.5 mm (0.020 in.) Stainless Steel	1060 C (1940 F)
MCS-6	0.5 mm (0.020 in.) Stainless Steel	1065 C (1949 F)
MCN-1	0.25 mm (0.010 in.) Nickel	960 C (1760 F)
MCN-2	0.25 mm (0.010 in.) Nickel	1055 C (1931 F)
MCN-3	0.25 mm (0.010 in.) Nickel	1045 C (1913 F)
MCN-4	0-0.75 mm (0.030 in.) Nickel	1035 C (1895 F)
MCN-5	0-0.75 mm (0.030 in.) Nickel	1013 C (1855 F)
MCN-6	0-0.75 mm (0.030 in.) Nickel	1100 C (1980 F)

ison with the specimens brazed during the Skylab flight, which were jointly analyzed by the Marshall Space Flight Center and experiment consultant personnel. One Exothermic Brazing Experiment assembly containing four tube and sleeve assemblies was reserved as a backup flight package or for use in tests to duplicate any unexpected conditions encountered during the flight experiment.

In addition, two nickel material specimens with a radioactive tracer 110-silver were brazed for the Oak Ridge National Laboratory personnel who developed the isotope mapping techniques subsequently applied to

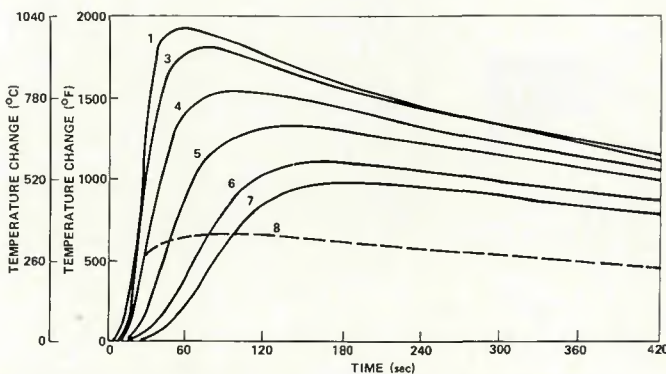


Fig. 6—Temperature profile curves of exothermic heating of tube

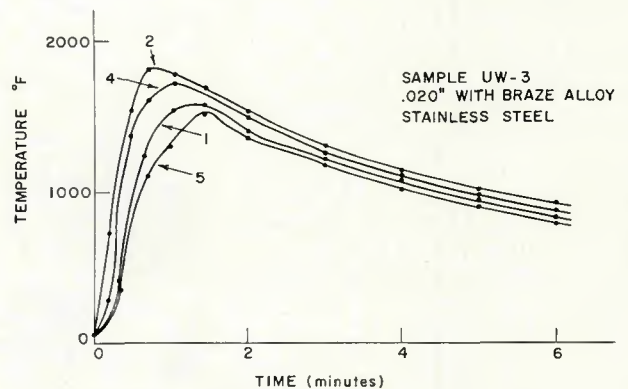


Fig. 7—Thermal cycle of sample UW-3

the Skylab specimens.^{2,3} Testing was also performed to assure the safety of the Skylab crew and photographic film relative to the radiation effect of the isotopes. Further, three specimens were brazed at Massachusetts Institute of Technology from which a thermal analysis for the experiment was derived.^{2,4}

Five samples of Skylab configuration were brazed after the flight at the University of Wisconsin to measure temperature gradients between the tube and sleeve and also to demonstrate that a warpage of the tube on the Skylab samples could be duplicated on the ground by simple end constraint.⁵

Other post-flight tests included the following:

1. A study on the effect of relative tube and sleeve motion at brazing temperatures by rotating a tube against the plate in the presence of molten braze alloy.

2. A study on the effect of centrifugal force on the segregation of phases during solidification by cooling a sample of braze alloy containing dissolved nickel under an artificial gravitational force.

3. An attempt to duplicate an abnormal microstructure (seen only in the Skylab nickel samples) by mixing braze alloy with small nickel particles and allowing the mixture to cool at a rate near that of the Skylab samples.⁵

Comparison of Skylab Brazing and Ground Reference

Engineering Results

SLS-1 [gap 0.13 mm (0.005 in.)—304L material] specimen montage X-ray is shown in Fig. 9 and is compared with a typical ground-brazed sample MCS-1 of the same configuration. The Skylab sample exhibited a nearly perfect braze joint. One minor shrinkage

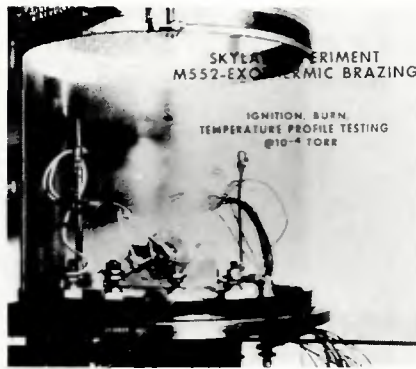


Fig. 8—Ignition, burn, temperature profile testing at $13.3322 \times 10^{-3} \text{ N/M}^2 (10^{-4} \text{ Torr})$

defect was present adjacent to a ring groove at station F. Excess braze alloy had flowed inwardly through the slits in the tube and pooled over and adjacent to these slits on the tube I.D. The braze material was free from oxide. The braze alloy had completely spread to the outermost ends of the sleeve.

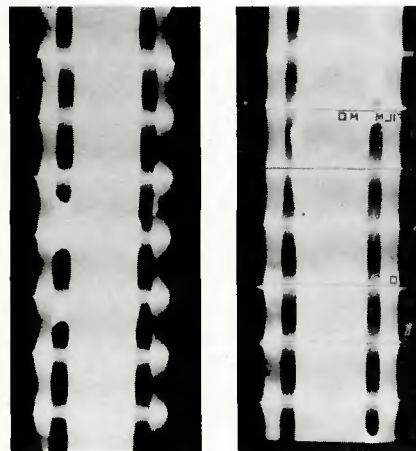


Fig. 10—Specimen montage radiographs (gap 0.25 mm, nickel material): A (left)—MCN-1 ground-brazed sample; B (right)—SLN-2 Skylab sample

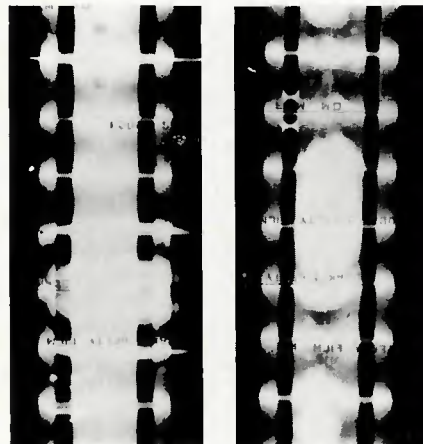


Fig. 9—Specimen montage radiographs (gap 0.13 mm, 304L material): A (left)—MCS-1 ground-brazed sample; B (right)—SLS-1 Skylab sample

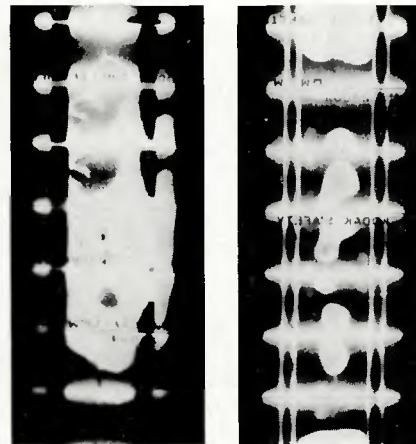


Fig. 11—Specimen montage radiographs (gap 0.5 mm, 304L material): A (left)—MCS-4 ground-brazed sample; B (right)—SLS-3 Skylab sample

MCS-1 was typical of the ground-brazed 0.13 mm (0.005 in.) gap characterization samples, all of which exhibited voids adjacent to ring grooves and a much higher frequency of small defects throughout the solidified braze zone. It should also be noted that a 0.13 mm (0.005 in.) gap exceeds normal design specification for braze joints in 1-g application. A normal design clearance for optimum capillary braze flow in 1-g would be approximately 0.05 mm (0.002 in.).

SLN-2 [gap 0.25 mm (0.010 in.)—nickel material] specimen montage X-ray is shown in Fig. 10 and is compared with a typical ground-brazed sample MCN-1 of the same configuration. In this specimen, the gap volume basically equals the volume of braze alloy. All specimens, Skylab and ground, retained some braze metal in the ring groove. This would indicate equalizing forces between the ring groove to retain the molten metal and the gap zone to draw the metal into it. Skylab and ground samples exhibited void areas in the braze gap zone.

SLS-3 [gap 0.5 mm (0.020 in.)—304L material] specimen montage is shown in Fig. 11 and is compared with a typical ground-brazed sample of the same configuration. This specimen was designed to represent a starved braze joint, possessing only half (50%) enough alloy to fill the 0.5 mm (0.020 in.) gap zone. Note that in the ground sample MCS-4, brazed in the horizontal position, all the braze metal had pooled at the bottom section, and gravity forces had completely drained the ring grooves. In contrast, the Skylab sample is a classic example of what happens when surface energy is the dominant force. A small quantity of braze alloy was retained as fillets in both ring grooves, and most braze alloy had bridged the 0.5 mm (0.020

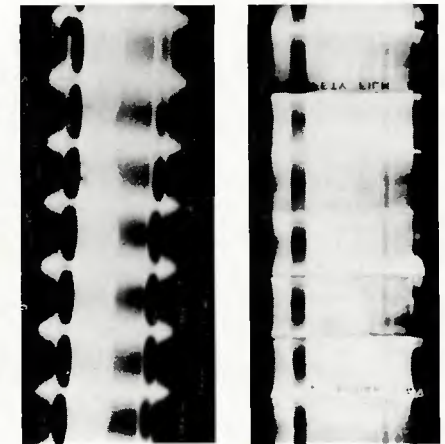


Fig. 12—Specimen montage radiographs (gap 0-0.75 mm, nickel material): A (left)—MCN-4 ground-brazed sample; B (right) SLN-4 Skylab sample

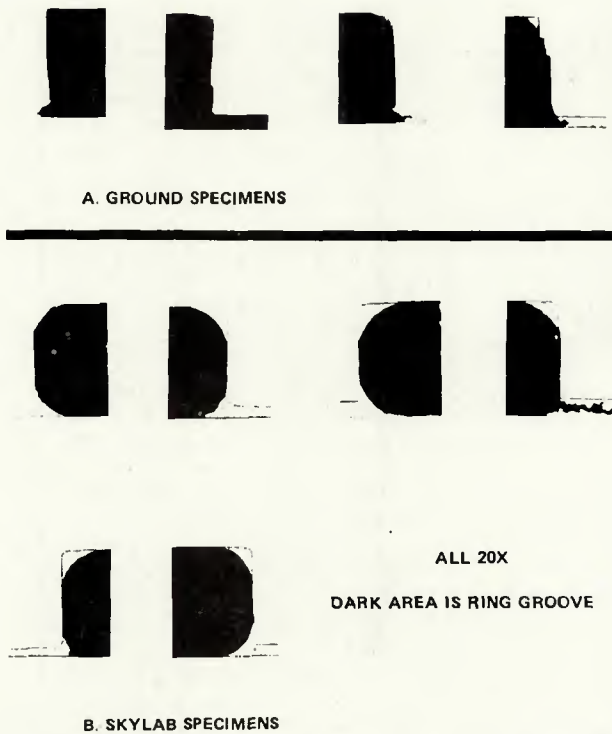


Fig. 13—Comparison of retained fillet in 304L ground-brazed specimen and Skylab specimen SL5-1

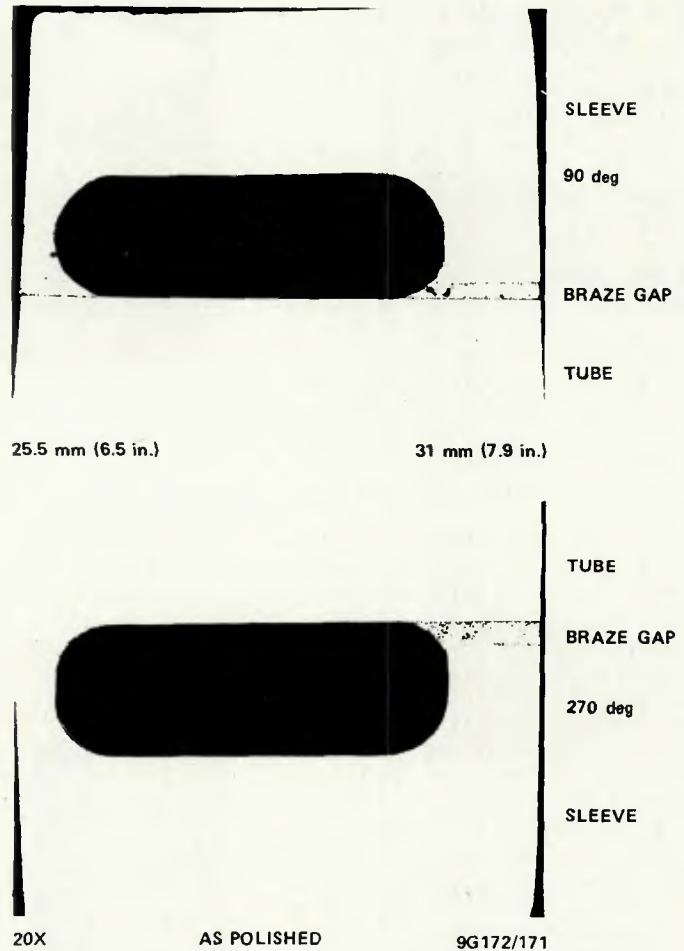


Fig. 14—Classic example of a braze material fillet retained in ring groove—Skylab specimen SLN-2. $\times 20$ (reduced 55% on reproduction)

in.) gap between the tube and sleeve. Some braze alloy was drawn through the three slits and pooled internally on the tube. The braze material in the Skylab sample is free from porosity and voids. It is logical to assume that the 0.5 mm (0.020 in.) gap would have completely filled had there been a sufficient amount of braze alloy.

SLN-4 [gap 0–0.76 mm (0–0.030 in.)—nickel material] specimen montage X-ray is shown in Fig. 12 and is compared with a typical ground-brazed sample MCN-4. The braze quality of the Skylab specimen was very good and much better than any ground-brazed characterization sample. Note that nearly all of the braze alloy was drawn from the SLN-4 ring groove at the left side of the photograph and at the narrow end of the gap. Braze alloy fillets on the ground and flight specimens were retained in the ring groove adjacent to the wide gap end. Variations in the contour lines of the braze alloy were caused by slight variations in concentricity between the sleeve and tube. Radioactive tracings indicate alloy spreading the full length of the sleeve, and some fillets of alloy were visible adjacent to the inserts at the wide end of the gap.

All the Skylab samples had the braze gaps filled to at least the same extent as the ground samples. Thus, this

design is capable of joining structures in the near-zero gravity environment of space with the assurance of the braze gaps filling as well as on Earth. One particular configuration gap 0.5 mm (0.020 in.) filled much better in Skylab and may have completely filled the gap if the design had included sufficient braze alloy.²

Joint pressure tightness of the two narrow Skylab samples was checked with a helium leak detector; they proved to be leak-free. Metallographic sectioning and study of the radiographs showed that the Skylab samples had a lower concentration of voids and braze defects than the corresponding ground samples.

Comparison of the radiographs for the Skylab wide gap stainless steel sample (SLS-3) with its ground characterization counterparts (Fig. 11) gives the best illustration of the effects of gravity. This sample, purposefully designed with insufficient braze alloy to fill the gap, was also designed with too large a gap to fill by capillary forces on Earth.

The radiograph of a typical ground sample in Fig. 11 indicates the braze alloy in both ring grooves melted and went to the lowest regions of the ring groove. This pressure head in the ring groove forced braze alloy into the interior of the tube through the

machined slits and out the ends of the tube. No braze alloy remained in the ring grooves, except at the bottom.

The radiograph of the Skylab sample in Fig. 11 indicates the ring grooves transferred braze alloy into the gap region where it was able to travel freely in the annular direction. The final position is shown by the three roughly circular "islands" in the gap region. The braze alloy remained in these three regions because the gap was slightly less in each of these regions due to upset caused by end constraint during heating. In contrast to the ground samples, over half of the braze alloy remained in the ring groove due to the relatively low driving force for the filling of such a large gap.

Scientific Results

Meniscus formation by the retention of braze alloy in the corners of the oversized ring grooves and fillets in the Skylab specimens was significantly different from the ground-based specimens. This observation clearly supports the relative enhancement of surface tension forces in a zero g field.⁶ This difference is shown in Fig. 13 of Skylab samples SLS-1 and a 304L stainless sample brazed on the ground. A typical retained fillet is shown in Fig.

14 of Skylab sample SLN-2, where complete fillet symmetry was obtained.

Visual and metallurgical examinations indicate the molten braze alloy spread farther and more uniformly in the constant gap Skylab samples, SLS-1, SLN-2 and SLS-3, than in the corresponding ground samples. A superior quality braze joint was noted in the SLS-1 sample. Thus, the predictions of improved capillary flow were confirmed.^{2,7} No firm conclusion was reached on the absence or presence of turbulence during capillary spreading in microgravity. Turbulence was expected to be possible only in Skylab specimens SLS-3 and SLN-4.

Ground characterization studies revealed that the oxygen partial pressure during brazing controlled the wetting and spreading of the braze alloy. An oxygen partial pressure of 1×10^{-4} Torr was found to inhibit the wetting and spreading of the braze alloy, while oxygen partial pressure as low as 3×10^{-5} Torr was found to measurably retard the wetting and spreading. Oxygen partial pressures below 1×10^{-5} Torr were found to have no effect on the wetting and spreading.⁵

110 Silver Tracer Application to Flow Patterns^{2,3}

Autoradiographs made from samples SLN-2 and SLN-4 are shown in Figs. 15 and 16. In these autoradiographs, the darker areas correspond to higher levels of radioactivity, and the 360 degree azimuth represents the circumference of the nickel sleeve. The original position of the tracer-containing pellet is marked on the print.

The autoradiograph for sample SLN-2 (Fig. 15) shows that the tracer alloy flowed mainly in a circumferential

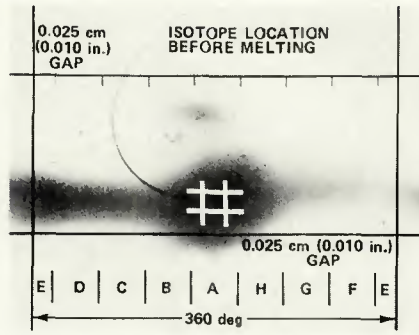


Fig. 15—Autoradiograph of Skylab specimen SLN-2

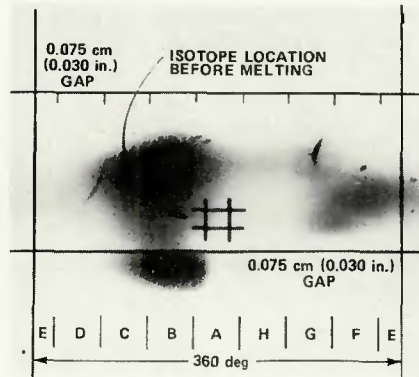


Fig. 16—Autoradiograph of Skylab specimen SLN-4

direction to areas at an azimuth of approximately 180 degrees from the original tracer pellet location A (0 deg). Most of the radioactivity is located in proximity to the original pellet location. An area of low radioactivity content can be seen just inside the tracer pellet location near the "upper" braze ring groove. After brazing in zero gravity, the tracer alloy in sample SLN-4 (Fig. 16) appeared to be concentrated in two areas—one above and the other below the tracer pellet location—although there was some

mixing of the isotope throughout the total taper-gap braze zone.

An explanation of the peripheral movement of the isotope in SLN-2 may be attributed to the melting and circumferential wetting of the small pellet of radioactive material before the melting of the remainder of the braze ring. It is emphasized that the radioactive pellet was not attached to the braze ring and therefore had minimal heat sink capability. Most of the melted radioactive material was retained within the ring groove, because the gap between the unmelted braze ring and the groove offered the best capillary path for movement of the melted pellet.

It is also believed that this condition occurred in sample SLN-4, i.e., the isotope pellet may have melted prior to the remaining portion of the braze ring. In this taper gap sample, the capillary attraction of the very narrow gap between the tube and sleeve, which was adjacent to the groove containing the pellet, was greater than that within the ring groove.

In summary, it is reasonable to believe that in SLN-2 and SLN-4 the isotope pellet melted before the major portion of the braze ring and moved by capillary attraction into the narrowest gap adjacent to it. Some additional mixing may have occurred between the radioactive material and the remaining braze rings when the latter melted and moved by capillary action into the narrower gap zones on both samples.³

Numerical Radioisotope Analysis

The first use of a radioisotope tracer for mapping flow patterns during brazing of metal components in a space environment (near-zero g) proved successful.^{2,3}

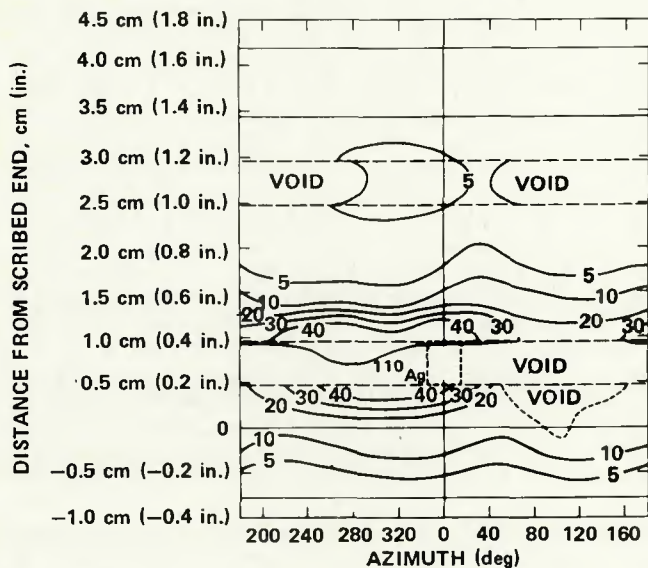


Fig. 17—Isotope intensity map—Skylab specimen SLN-2

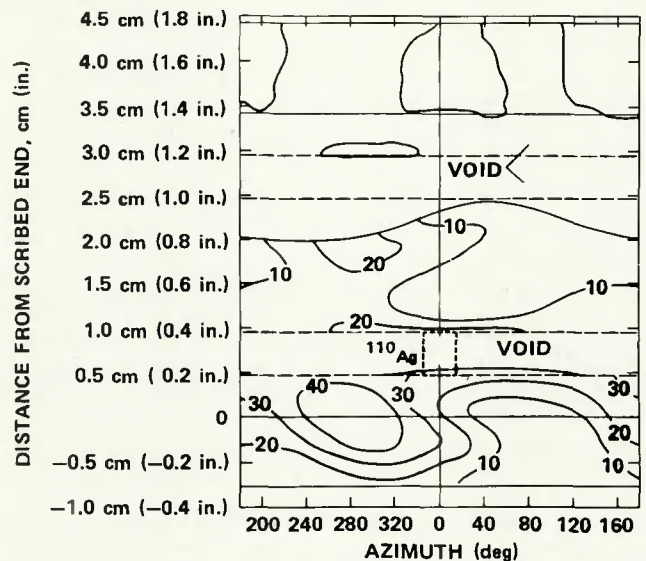


Fig. 18—Isotope intensity map—Skylab specimen SLN-4

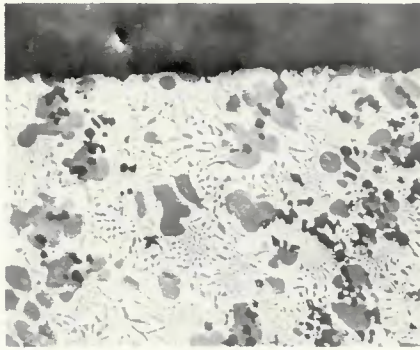


Fig. 19—Stainless steel particles in the braze alloy near the stainless steel-braze alloy interface in a ring groove—Skylab specimen SLS-3. $\times 500$ (reduced 46% on reproduction)

Radioisotope tracing consisted of measuring the intensity of radiation from the silver isotope at numerous points around the braze-filled annulus at many transverse sections of the tube. Individual radiation intensity results for all sections were then combined to generate a two-dimensional radiation intensity map of the entire braze joint. These maps are reproduced as Figs. 17 and 18.

In both ground and near-zero g experiments, there is evidence of braze material flowing into temperature "hot zones," generated by uneven ignition of the exotherm during the initial stages of the braze. This phenomenon would not have been observed without the use of the radioisotope tracer-containing alloy.

It is interesting to note that the areas void of solid braze alloy, yet wet by molten braze material, showed no residual tracer isotope activity. This observation would imply that the silver neither reacted with nor adhered to the nickel surface.

The silver-110 tracer maps for this experiment suggest that such tracing can provide a picture of the thermal history for any particular assembly, as well as accurate braze alloy flow information. Since no other analytical technique would provide this unique composite view of surface, gravitational and thermal forces, radioisotope tracing proved useful in interpreting other metallurgical aspects of this experiment.

The radiation intensity map for sample SLN-2 is shown in Fig. 17. This sample had a nominal annulus clearance of 0.25 mm (0.010 in.). Some of the braze alloy flowed outside the nickel ferrule in the samples brazed in space. The effect of this extraneous flow is also shown by the movement of the tracer alloy, which extended outside the zero reference plane to areas with negative distance values. However, most of the tracer alloy was concentrated on either side of the ring groove from an azimuth of approxi-

Table 3—Bulk Materials Balance for Braze Alloy in Specimen SLS-3

Region	Description	Volume, cu mils	Composition,		Volume copper, cu mils
			wt % Cu	at. % Cu	
1	Upper ring groove	6.25×10^6	36	39.6	2.475×10^6
2	Island in gap region	6×10^6	12	13.9	$.834 \times 10^6$
3	Island in gap region	1.6×10^6	14	16	$.256 \times 10^6$
3A	Copper region in island	9×10^4	80	82.5	$.07 \times 10^6$
4	Island in gap region	9×10^4	14	16	$.14 \times 10^6$
5	Lower ring groove	8.7×10^6	33	36.6	3.18×10^6
	Total	23.55×10^6 ^(a)		Total	6.95×10^6 ^(b)

^(a) 23.55×10^6 cubic mils = 3.86×10^{-1} cm³, 3.86×10^{-1} cm³ $\times 10.08$ average density = 3.89 g \approx 3.9 g placed in originally.

^(b) $6.95 \times 10^6 / 23.55 \times 10^6 = 29.5$ at. % Cu = 27 wt. % Cu \approx 28 wt. % Cu specified in bulk braze alloy.

mately 40 deg, moving to the left to 200 deg. An area of slight activity was found in the "upper" ring groove associated with a fillet of braze material. These results agree with those observed in the autoradiograph for sample SLN-2, showing high radioisotope content along the "lower" ring groove.

The radiation intensity map for sample SLN-4, having a 0-0.76 mm (0-0.030 in.) taper annulus, is shown in Fig. 18. The braze extended beyond the nickel ferrule, and moderate concentrations of the radioisotope were detected outside the ferrule edge at negative distance values. However, most of the silver-110 tracer isotope was concentrated in the area above and below the tracer ring groove at an azimuth of approximately 280 deg. Since SLN-4 was a taper gap sample, it must again be noted that the lower concentration area inside the ring groove actually gave higher radiation intensity values than the high concentration area outside the groove, but these latter values were normalized by dividing by a smaller volume increment. With this normalization in mind, comparison of the tracer map in Fig. 18 can be made to the autoradiograph in Fig. 16. The map and autoradiograph show the presence of two regions of intense radioactivity, and they agree with respect to their azimuthal location.³

Microstructural Features

Comparison of the Skylab and ground characterization samples revealed proeutectic dendrites that had

formed with the same shape and arm spacing. Also, the eutectic structure was unaffected by the change in gravitational field.^{2,6} In addition to these similarities, there were a number of differences between the Skylab and ground samples.

SLS-7: Stainless steel particles were dispersed in the braze alloy at a concentration three times higher than in the ground-processed samples.

SLN-2: A unique structure appeared in some regions in which a globular copper-nickel second phase was observed in a matrix silver phase with the globular phase present at between 30 and 90 volume percent. The globular structure was much different than the ground samples and other regions of the Skylab sample—Fig. 19.

SLS-3: Compared to the ground samples, the proeutectic silver-rich phase was more noticeable in the gap region, while the grooves where the braze alloy had been preplaced were copper-rich. Table 3, a schematic of the final braze alloy distribution, denotes one "island" of braze alloy that contained about 11% copper near the edges and 80% copper near the center. The stainless steel particle concentration was about ten times that of the respective ground-processed samples.

SLN-4: A globular copper-nickel phase not found in the ground samples was present in the narrow gap end. Presence of proeutectic silver-rich phase not found in ground samples was noted.

A curious feature of the stainless steel specimens was the presence of finely dispersed stainless steel particles

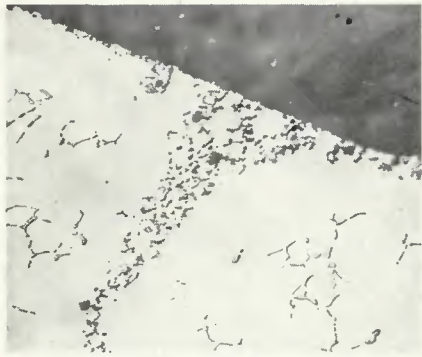


Fig. 20—Stainless steel particles in the silver-rich braze alloy in the gap region—Skylab specimen SLS-3. $\times 250$ (reduced 46% on reproduction)

within the braze alloy.^{2,6} The first inclination is to attribute these particles to the presence of debris remaining from machining the specimens. However, the specimens were very thoroughly cleaned, and the particles are extremely small, ranging from 0.5 to 5.0 μm (0.000020 to 0.002 in.) in diameter. Stainless steel does not readily fragment into such fine particles; it is more likely these inclusions (Figs. 20 and 21) are the consequences of erosive attack of the stainless steel by the liquid metal. This is taken as still further evidence of the vigorous flow peculiar to the Skylab specimens, as the particles were detected in the ground characterization specimens at only one-tenth to one-third the concentration. Since the particles were also produced in the ground-based samples, their presence was obviously not a near-zero g effect.⁵

Formation of the globular copper-nickel phase was made possible by a high concentration of nickel particles removed by the same mechanisms of fluid flow and contact between the tube and sleeve observed in the Skylab stainless steel specimens. The resultant nickel concentrations were above the solubility limit for the silver-copper eutectic, and thus many particles remained at equilibrium. In comparison, the lower concentration of particles in the ground samples went into solution completely. Examination of phase relationships in this system indicates that the globular copper-nickel phase and reduced amount of eutectic are results of the higher dissolved nickel concentrations and retained nickel particles in the Skylab nickel samples.⁵

The binary silver-copper alloy without nickel separated upon solidification into two solid phases: one rich in copper but containing some dissolved silver, and the other rich in silver containing some dissolved copper. When nickel is added to the silver-copper alloy, the nickel preferentially associates with the copper-rich phase



Fig. 21—A (left)—normal structure in some regions of Skylab nickel specimens and all ground-brazed specimens; B (right)—abnormal structure seen in other regions of the Skylab specimens. $\times 500$ (reduced 28% on reproduction)

upon solidification, being quite insoluble in the silver-rich phase. Moreover, silver and nickel appear to be mutually exclusive in the copper-rich phase. In fact, two kinds of copper-rich phase form, one containing nickel but no silver, and the other containing silver but almost no nickel.

The solidification process is rendered quite complicated by the addition of nickel. The simple binary 72% silver/28% copper freezes substantially at one temperature, 780 C (1436 F), and the product of solidification exhibits the classical eutectic structure, a finely dispersed mechanical mixture of silver-rich and copper-rich phases. The presence of nickel increases the temperature at which solidification begins, and the first solid crystals which form contain copper and nickel with practically no silver. These crystals become fairly large before the rest of the alloy freezes at approximately 780 C (1436 F).

These large copper-nickel crystals (or dendrites) are called primary, because they form first upon cooling. Some primary copper-rich dendrites were also observed in the stainless steel specimens, but these contained much less nickel, because the specimens contained only eight percent nickel. As more and more nickel dissolves in the silver-copper alloy, the fine eutectic structure progressively, and finally completely, disappears. Very abnormal structures, surprisingly high in nickel concentration, were observed only in the Skylab samples.

The first effect of dissolved nickel is to increase the temperature at which solidification begins: a copper-rich

primary phase containing nickel forms at a temperature well above 780 C (1436 F). Upon cooling, when the temperature begins to approach 780 C (1436 F), virtually all the nickel is rejected from the liquid solution because it is virtually insoluble in the silver-rich liquid at temperatures below 850 C (1572 F). Thus, it is the nickel which causes the primary copper phase to form at a relatively high temperature; however, this primary crystallization has the effect of removing copper from the liquid. The remaining liquid contains appreciably more than 72% silver, and primary silver-rich phase now must form at a temperature slightly above 780 C (1436 F). When the eutectic temperature, 780 C (1436 F), is finally reached, whatever liquid still remains contains very nearly 72% silver/28% copper and freezes to a fine eutectic structure.

If the initial nickel concentration in the liquid is high enough, solidification will become nearly complete at a temperature above 780 C (1436 F), and no normal eutectic structure will form. "The two-phase field resulting from the silver-copper-eutectic decomposition terminates with the addition of 5 weight percent nickel."¹⁰ The quotation is an interpretation of early work done on the silver-copper-nickel ternary system,¹¹ and is qualitatively correct.

Skylab sample SLS-3 was found to contain a silver-rich structure in the gap region containing only 11-14% copper compared to the initial 28% copper.^{2,6} During the search for this missing copper, the sample was sectioned through one small dark spot

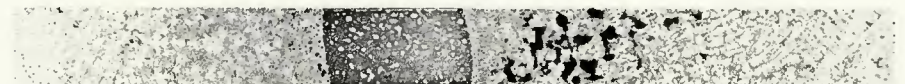


Fig. 22—Section through a copper-rich region in Skylab specimen SLS-3. The light region on each end is silver-rich. $\times 80$ (enlarged 11% on reproduction)

seen on the radiograph. This spot, illustrated in Fig. 22 by a cross-section, was analyzed as containing over 80% copper in the center⁵ and was formed by rotation of the island during solidification. As the rotating island cooled, the proeutectic copper phase solidified and moved to the center of the island because of its lower density. The proeutectic silver phase formed next and stopped the rotation of the island. Last to solidify was a small band of eutectic composition liquid between the central copper-rich region and the silver-rich region, and so this eutectic band contains solidification shrinkage.

The copper contained in this spot was insufficient to offset the high silver-rich content of the islands and makes the overall composition eutectic. A continued search for the missing copper revealed that the braze alloy retained in both ring grooves was copper-rich. A materials balance was done in the braze alloy and indicated the overall composition was that of the eutectic—Table 3.⁵ Formation of the copper-rich spot was successfully simulated on Earth by centrifuging the solidifying alloy.⁵

Summary

This experiment conclusively demonstrated the utility of brazing as a joining method in the near-zero gravity experienced in the Skylab flights. The joints were of a higher quality than the corresponding ground samples in terms of defects and porosity.

No apparent upper limit to the braze gap exists so that joints with large fit-up tolerances are possible. However, a better braze alloy feeding design would be necessary for wide gap joints, as only about half of the braze alloy was transferred to the gap from the ring groove on the Skylab 0.5 mm (0.020 in.) gap sample.

Meniscus shape on the Skylab samples was in close agreement to what had been expected. The surface tension of the liquid silver-copper alloy appears to be independent of the lithium content.

Wetting and spreading in Skylab seems to have been better than on the ground samples. This was expected due to the pumping capabilities of space and the absence of the oil film which was present on the surface of the ground specimens prepared in a diffusion pumped system. An oxygen partial pressure of 1×10^{-4} Torr was found to inhibit wetting of the stainless steel by the braze alloy. Isotope mapping successfully revealed flow pattern in the braze joints.

There were distinct similarities in microstructure between the ground and Skylab samples, indicating the unimportance of gravity on the atomic level. Differences that were observed in the microstructure have been attributed to the greater freedom of motion for the molten braze alloy, which resulted in the segregation of a copper-rich region in SLS-3 and the generally higher particle concentration from erosion of base metal in the braze alloy of all the Skylab samples.

References

1. Skylab, *Materials Processing in Space Experiments M-512, M-551, M-552, M-553, M-554, M-555*, NASA, May (1972).
2. *Proceedings: Third Space Processing Symposium: Skylab Results*, NASA, April 30-May 1 (1974).
3. Braski, D.N., Adair, H.L., and Kobisk, E.H., *Radioisotope Tracer Studies in the NASA Skylab Exothermic Brazing Experiment M-552*, Oak Ridge National Laboratory, Contract No. W-74-5-eng-26 (1973).
4. Musaki, T., and Masabuchi, K., *Thermal Analysis of M552 Experiment for Materials Processing in Space*, Massachusetts Institute of Technology Contractor Report (1973).
5. Siewert, T., *A Study of Brazing in Skylab II*, Thesis (1976).
6. Heine, R.W., Adams, Jr., C.M., and Siewert, T.A., *Report on Flight/Ground Sample Comparison Relating to Flight Experiment M-552, Exothermic Brazing*, University of Wisconsin Contractor Report (1973).
7. Pattee, H.E., and Monroe, R.E., *Characterization of Exothermic Brazing Components, Skylab Sample M-552*, Battelle Columbus Laboratories Contractor Report (1973).
8. Tobin, J.M., and Kossowsky, R., *Research Study on Materials Processing in Space Experiment No. 512, Final Report on M-551, M-552, M-553*, Westinghouse Astronuclear Laboratory, WANL-L-854 (1973).
9. Bourgeois, Jr., S.V., *Convection in Skylab M-512, Experiments M-551, M-552, and M-553, Phase B Report*, Lockheed Huntsville R&E Center, LM SE-HREC TR D306697 (1973).
10. *Metals Handbook*, 8, p. 380, (1973).
11. Guertler, W., and Bergmann, A., "Study of the Ternary Ag-Cu-Ni," *Zeitschrift für Metallkunde*, 25, 53, (1933).

WRC Bulletin 228

July 1977

Statistical Analysis of Dependence of Weld Metal Properties on Composition

by J.A. Marshall and J. Heuschkel

The weld metal development programs described herein were carried out at the Westinghouse Research and Development Center in a series of programs spanning about 25 years. This led to the accumulation of a substantial body of data which now provides the basis for relating mechanical properties of weld metal to weld metal chemistry. They are brought together in this Bulletin for statistical analysis. The results of this analysis should be useful in planning, expressing, comparing and interpreting future experimental programs on weld development.

Publication of this paper was sponsored by the Weldability (Metallurgical) Committee of the Welding Research Council.

The price of WRC Bulletin 228 is \$8.50 per copy. Orders should be sent with payment to the Welding Research Council, United Engineering Center, 345 East 47th Street, New York, NY 10017.